

## DUAL HIGGS THEORY FOR COLOR CONFINEMENT

H. ICHIE

*Department of Physics, Tokyo Institute of Technology  
Meguro, Tokyo 152-8551, Japan  
E-mail: ichie@th.phys.titech.ac.jp*

H. SUGANUMA

*Research Center for Nuclear Physics (RCNP), Osaka University  
Ibaraki, Osaka 567-0047, Japan*

We study theoretical bases of the dual Higgs theory for confinement physics in QCD in terms of monopoles and the gluon configuration in the maximally abelian (MA) gauge. Abelian dominance for the confinement force can be analytically proved by regarding the off-diagonal angle variable as a random variable in the lattice formalism. In the long-distance scale, the contribution of off-diagonal gluons to the Wilson loop cancels each other and exhibits a perimeter law behavior, which leads to exact abelian dominance on the string tension if the finite size effect of the Wilson loop is removed. We investigate the appearance of the monopole in the QCD vacuum, considering the role of off-diagonal gluons. The monopole carries a large fluctuation of the gluon field and provides a large abelian action in abelian projected QCD. Due to the partial cancellation between the abelian part and the off-diagonal part of the QCD action, the monopole can appear in QCD without large cost of the QCD action. The off-diagonal gluon is necessary for existence of the monopole at the short-distance scale. We study monopole condensation, which is the requirement of the dual Higgs theory, by comparing the QCD vacuum with the monopole-current system. We find that “entropy” of monopole-current dominates than its “energy”, and the monopole seems to be condensed at the infrared scale in the QCD vacuum.

### 1 Dual Superconductor Picture for Confinement in QCD

The strong interaction is subjected to Quantum Chromodynamics (QCD). Due to the self-interaction of the gauge field, the QCD gauge coupling becomes very strong in the low-energy region, while it is weak in the high-energy region. Accordingly, QCD phenomena are divided into two theoretical categories: the strong coupling leads to complicated nonperturbative phenomena such as color confinement and chiral symmetry breaking, while high-energy phenomena are understood by the perturbative QCD. Since there is no well-established analytical method for nonperturbative phenomena, one must carry out the Monte Carlo simulation based on the lattice QCD or apply the effective models described by the relevant degrees of freedom for the low-energy physics. As for the chiral dynamics, the pion and the sigma meson, which are composite modes of quark and anti-quark, play an important role for the infrared effective theory

such as the (non-)linear sigma model and the Nambu-Jona-Lasinio model. On the other hand, confinement is essentially described by the dynamics of gluons rather than quarks.

In 1970's, Nambu proposed an interesting idea that quark confinement can be interpreted using the dual version of the superconductivity<sup>1</sup>. In the superconductor, Cooper-pair condensation leads to the Meissner effect, and the magnetic flux is squeezed like a quasi-one-dimensional tube as the Abrikosov vortex. On the other hand, from the Regge trajectory of hadrons and the lattice QCD, the confinement force between the color-electric charge is brought by one-dimensional squeezing of the color-electric flux in the QCD vacuum. Hence, the QCD vacuum can be regarded as the dual version of the superconductor. In this dual-superconductor picture for the QCD vacuum, the squeezing of the color-electric flux between quarks is realized by the dual Meissner effect as the result of condensation of color-magnetic monopoles. However, there are two large gaps between QCD and the dual superconductor picture.

1. This picture is based on the abelian gauge theory, while QCD is a non-abelian gauge theory.
2. The dual-superconductor scenario requires condensation of magnetic monopoles as the key concept, while QCD does not have such a monopole as the elementary degrees of freedom.

As the connection between QCD and the dual superconductor scenario, 't Hooft proposed the concept of the abelian gauge fixing<sup>2</sup>, the partial gauge fixing which is defined so as to diagonalize a suitable gauge-dependent variable  $\Phi[A_\mu(x)]$ . The abelian gauge fixing reduces QCD into an abelian gauge theory, where the off-diagonal element of the gluon field behaves as a charged matter field (See Fig.1). As a remarkable fact in the abelian gauge, color-magnetic monopoles appear as topological objects corresponding to the nontrivial homotopy group  $\Pi_2(\mathrm{SU}(N_c)/\mathrm{U}(1)^{N_c-1}) = \mathbf{Z}_\infty^{N_c-1}$ . Here, we assume abelian dominance, which means that the only abelian gauge fields with monopoles would be essential for the description of the nonperturbative QCD, and neglect the off-diagonal elements, which is called

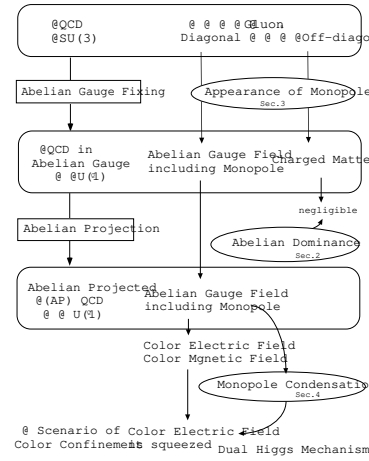


**Fig.1** Dual Superconductor Picture  
in QCD

abelian projection. Thus, by the abelian gauge fixing and the abelian projection, QCD is reduced into abelian projected (AP-)QCD, which is abelian gauge theory including monopoles. If the monopole condenses, the scenario of color confinement by the dual Meissner effect would be a realistic picture for confinement in QCD. In this paper, using the lattice QCD simulation, we study the key of the dual Higgs theory: abelian dominance (Sec.2), the appearance of monopole (Sec.3) and monopole condensation (Sec.4).

## 2 Abelian Dominance in the Maximally Abelian Gauge

Abelian dominance on the confinement force has been investigated using the lattice QCD simulation in the maximally abelian (MA) gauge<sup>3,4</sup>. In terms of the link variable  $U_\mu(s) \equiv U_\mu^0(s) + i\tau^a U_\mu^a(s)$ , the MA gauge fixing is defined by maximizing  $R \equiv \sum_{s,\mu} \text{tr}(U_\mu(s)\tau_3 U_\mu^\dagger(s)\tau_3) = \sum_{s,\mu} \{(U_\mu^0(s))^2 + (U_\mu^3(s))^2 - (U_\mu^1(s))^2 - (U_\mu^2(s))^2\}$  through the gauge transformation. In this gauge, the off-diagonal components,  $U_\mu^1$  and  $U_\mu^2$ , are forced to be small, and therefore the QCD system seems describable by U(1)-like variables approximately. It is to be noted that the MA gauge is a sort of the abelian gauge, because  $\Phi(s) \equiv \sum_{\mu,\pm} U_{\pm\mu}(s)\tau_3 U_{\pm\mu}^\dagger(s)$  is diagonalized there. (For the simple notation, we use  $U_{-\mu}(s) \equiv U_\mu^\dagger(s-\mu)$  in this paper). In this section, we study the origin of abelian dominance on the confinement force in the QCD vacuum, considering the relation to abelian dominance on the link variable.

### 2.1 Abelian Dominance on Link Variable: Microscopic Abelian Dominance

In the lattice formalism, the SU(2) link variable  $U_\mu(s)$  is factorized as

$$U_\mu(s) = \begin{pmatrix} \cos\theta_\mu(s) & -\sin\theta_\mu(s)e^{-i\chi_\mu(s)} \\ \sin\theta_\mu(s)e^{i\chi_\mu(s)} & \cos\theta_\mu(s) \end{pmatrix} \begin{pmatrix} e^{i\theta_\mu^3(s)} & 0 \\ 0 & e^{-i\theta_\mu^3(s)} \end{pmatrix} \equiv M_\mu(s)u_\mu(s),$$

where  $u_\mu(s)$  and  $M_\mu(s)$  correspond to the diagonal part and the off-diagonal part, respectively. For the residual U(1)<sub>3</sub> gauge transformation,  $u_\mu(s)$  behaves as the abelian gauge field, while  $c_\mu(s)$  behaves as the charged matter. Here, the range of angle variables are taken as  $0 \leq \theta_\mu \leq \frac{\pi}{2}$ ,  $-\pi \leq \theta_\mu^3, \chi_\mu < \pi$ .

In order to investigate abelian dominance on the link variable in the MA gauge, we define ‘‘abelian projection rate’’ as  $R_{\text{Abel}}(s, \mu) \equiv \cos\theta_\mu(s)$ . For instance, if  $\cos\theta_\mu = 1$ , the SU(2) link variable is completely abelian as  $U_\mu(s) = \begin{pmatrix} e^{i\theta_\mu^3} & 0 \\ 0 & e^{-i\theta_\mu^3} \end{pmatrix}$ , while it is off-diagonal as  $U_\mu(s) = \begin{pmatrix} 0 & -e^{-i(\theta_\mu^3+\chi_\mu)} \\ e^{i(\theta_\mu^3+\chi_\mu)} & 0 \end{pmatrix}$  if  $\cos\theta_\mu = 0$ . We show in Fig.2 the spatial distribution of the abelian projection rate  $R_{\text{Abel}} = \cos\theta$  as an arrow ( $\sin\theta, \cos\theta$ ). In the MA gauge, most of all SU(2) link variables become U(1)-like. We show also in Fig.3 the probability

distribution  $P(R_{\text{Abel}})$  of the abelian projection rate  $R_{\text{Abel}}$ . Without gauge fixing, the average  $\langle R_{\text{Abel}} \rangle$  is found to be about  $\frac{2}{3}$ . In the MA gauge, the off-diagonal component of the  $SU(2)$  link variable is forced to be reduced, and  $R_{\text{Abel}}$  approaches to unity; one obtains  $\langle R_{\text{Abel}} \rangle_{\text{MA}} \simeq 0.93$  on  $16^4$  lattice with  $\beta = 2.4$ . Thus, we find *microscopic abelian dominance* on the link variable.

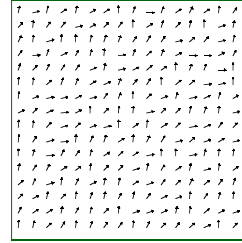
## 2.2 Analytical Study on Abelian Dominance for Confinement : Macroscopic Abelian Dominance

In this section, we study the origin of abelian dominance on the confinement force, considering the relation with *microscopic abelian dominance* on the link variable<sup>5</sup>. In the MA gauge, the diagonal element  $\cos \theta_\mu(s)$  in  $M_\mu(s)$  is maximized by the gauge transformation as large as possible;  $R_{\text{Abel}} = 0.93$  at  $\beta = 2.4$ . Then, the *off-diagonal element*  $e^{i\chi_\mu(s)} \sin \theta_\mu(s)$  is forced to take a small value in the MA gauge, and therefore the approximate treatment on the off-diagonal element would be allowed in the MA gauge. Moreover, the *angle variable*  $\chi_\mu(s)$  is not constrained by the MA gauge-fixing condition at all, and tends to take a random value besides the residual  $U(1)_3$  gauge degrees of freedom. Hence,  $\chi_\mu(s)$  in the MA gauge can be regarded as a *random angle variable* in a good approximation.

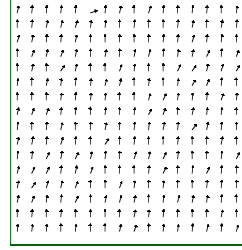
Let us consider the Wilson loop  $\langle W_C[U_\mu(s)] \rangle \equiv \langle \text{tr} \Pi_C U_\mu(s) \rangle$  in the MA gauge. In calculating  $\langle W_C[U_\mu(s)] \rangle$ , the expectation value of  $e^{i\chi_\mu(s)}$  in  $M_\mu(s)$  vanishes as  $\langle e^{i\chi_\mu(s)} \rangle_{\text{MA}} \simeq \int_0^{2\pi} d\chi_\mu(s) \exp\{i\chi_\mu(s)\} = 0$ , when  $\chi_\mu(s)$  is assumed to be a *random angle variable*. Then, the off-diagonal factor  $U_\mu(s)$  appearing in the Wilson loop  $W_C[U_\mu(s)]$  becomes a diagonal matrix,  $U_\mu(s) \equiv M_\mu(s)u_\mu(s) \rightarrow \cos \theta_\mu(s)u_\mu(s)$ , in the MA gauge.

Then, for the  $I \times J$  rectangular  $C$ , the Wilson loop  $W_C[U_\mu(s)]$  in the MA gauge is approximated as

$$\begin{aligned} \langle W_C[U_\mu(s)] \rangle &\equiv \langle \text{tr} \prod_{i=1}^L U_{\mu_i}(s_i) \rangle \simeq \langle \prod_{i=1}^L \cos \theta_{\mu_i}(s_i) \cdot \text{tr} \prod_{j=1}^L u_{\mu_j}(s_j) \rangle_{\text{MA}} \\ &\simeq \langle \exp\{\sum_{i=1}^L \ln(\cos \theta_{\mu_i}(s_i))\} \rangle_{\text{MA}} \langle W_C[u_\mu(s)] \rangle_{\text{MA}} \\ &\simeq \exp\{L \langle \ln(\cos \theta_\mu(s)) \rangle_{\text{MA}}\} \langle W_C[u_\mu(s)] \rangle_{\text{MA}}, \end{aligned} \quad (1)$$



(a) No Gauge Fixing



(b) MA Gauge Fixing

**Fig.2** Local abelian projection rate  $R_{\text{Abel}} = \cos \theta$  at  $\beta = 2.4$  on  $16^4$  lattice. Arrows denote  $(\sin \theta, \cos \theta)$   $[0 \leq \theta \leq \frac{\pi}{2}]$ .

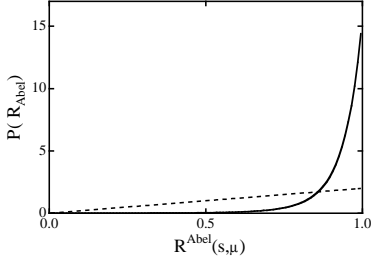


**Fig.3** The probability distribution  $P(R_{\text{Abel}})$  of abelian projection rate  $R_{\text{Abel}}(s, \mu)$  at  $\beta = 2.4$  on  $16^4$  lattice from 40 gauge configurations in the MA gauge (solid curve) and without gauge fixing (dashed curve).

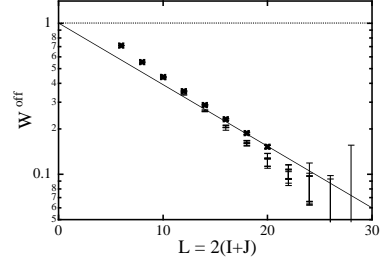


**Fig.4** The comparison between the analytical estimation (straight line) and the lattice data ( $\times$ ) of  $W_C^{\text{off}} \equiv \langle W_C[U] \rangle / \langle W_C[u] \rangle_{\text{MA}}$  with  $I, J \geq 2$  as the function of the perimeter  $L \equiv 2(I + J)$  in the MA gauge at  $\beta = 2.4$ .

where  $L \equiv 2(I+J)$  denotes the perimeter length and  $W_C[u_\mu(s)] \equiv \text{tr} \Pi_{i=1}^L u_{\mu_i}(s_i)$  the abelian Wilson loop. Here, we have replaced  $\sum_{i=1}^L \ln \{ \cos(\theta_{\mu_i}(s_i)) \}$  by its average  $L \langle \ln \{ \cos(\theta_{\mu_i}(s)) \} \rangle_{\text{MA}}$  in a statistical sense. In this way, we derive a simple estimation as  $W_C^{\text{off}} \equiv \langle W_C[U_\mu(s)] \rangle / \langle W_C[u_\mu(s)] \rangle_{\text{MA}} \simeq \exp \{ L \langle \ln(\cos \theta_\mu(s)) \rangle_{\text{MA}} \}$  for the *contribution of the off-diagonal gluon element to the Wilson loop*. From this analysis, the contribution of off-diagonal gluons to the Wilson loop is expected to obey the *perimeter law* in the MA gauge for large loops, when the statistical treatment would be accurate.

In the lattice QCD, we find that  $W_C^{\text{off}}$  seems to obey the *perimeter law* for the Wilson loop with  $I, J \geq 2$  in the MA gauge, as shown in Fig.4. We find also that the lattice results on  $W_C^{\text{off}}$  as the function of  $L$  is well reproduced by the above estimation with *microscopic information* on the diagonal factor  $\cos \theta_\mu(s)$  as  $\langle \ln \{ \cos_\mu(s) \} \rangle_{\text{MA}} \simeq -0.082$  for  $\beta = 2.4$ .

Thus, the off-diagonal contribution  $W_C^{\text{off}}$  to the Wilson loop obeys the perimeter law in the MA gauge, and therefore the SU(2) string-tension  $\sigma_{\text{SU}(2)}$  becomes same as the abelian string-tension  $\sigma_{\text{Abel}}$ ,

$$\begin{aligned} \sigma_{\text{SU}(2)} &\equiv - \lim_{I, J \rightarrow \infty} \frac{1}{IJ} \ln \langle W_{I \times J}[U_\mu(s)] \rangle \\ &\simeq -2 \langle \ln \{ \cos \theta_\mu(s) \} \rangle_{\text{MA}} \lim_{I, J \rightarrow \infty} \frac{I+J}{IJ} + \sigma_{\text{Abel}} \xrightarrow{I, J \rightarrow \infty} \sigma_{\text{Abel}}, \end{aligned} \quad (2)$$

when the finite size effect on  $I$  and  $J$  is removed. Thus, *abelian dominance for the string tension*,  $\sigma_{\text{SU}(2)} = \sigma_{\text{Abel}}$ , can be proved in the MA gauge by replacing the off-diagonal angle variable  $\chi_\mu(s)$  as a random variable.

### 3 Monopoles in QCD

In this section, we derive the abelian gauge theory including monopoles in terms of the gauge connection, and study monopole properties<sup>6</sup>.

In the general system including singularities such as the Dirac string, the field strength is defined as  $G_{\mu\nu} \equiv \frac{1}{ie}([\hat{D}_\mu, \hat{D}_\nu] - [\hat{\partial}_\mu, \hat{\partial}_\nu])$  with the covariant derivative  $\hat{D}_\mu \equiv \hat{\partial}_\mu + ieA_\mu$ . By the general gauge transformation with the gauge function  $\Omega$ , the field strength  $G_{\mu\nu}$  is transformed as

$$\begin{aligned} G_{\mu\nu} \rightarrow G_{\mu\nu}^\Omega &= \Omega G_{\mu\nu} \Omega^\dagger = (\partial_\mu A_\nu^\Omega - \partial_\nu A_\mu^\Omega) + ie[A_\mu^\Omega, A_\nu^\Omega] + \frac{i}{e} \Omega [\partial_\mu, \partial_\nu] \Omega^\dagger \\ &\equiv G_{\mu\nu}^{\text{linear}} + G_{\mu\nu}^{\text{bilinear}} + G_{\mu\nu}^{\text{sing}}. \end{aligned} \quad (3)$$

The last term  $G_{\mu\nu}^{\text{sing}}$  remains only for the singular gauge transformation, and can provide the Dirac string.

Here, in order to study appearance of the monopole, let us consider the SU(2) singular gauge-function  $\Omega = \begin{pmatrix} e^{i\varphi} \cos \frac{\theta}{2} & \sin \frac{\theta}{2} \\ -\sin \frac{\theta}{2} & e^{-i\varphi} \cos \frac{\theta}{2} \end{pmatrix}$  with polar angle  $\theta$  and azimuthal angle  $\varphi$ . Here,  $\Omega$  is multi-valued at the positive region of  $z$ -axis,  $\theta = 0$ , and the last term  $G_{\mu\nu}^{\text{sing}}$  in Eq.(3) provides the singular gauge configuration of the Dirac string in the abelian sector, as shown in Fig.5. Accordingly, the linear term  $G_{\mu\nu}^{\text{linear}}$  and the second term  $G_{\mu\nu}^{\text{bilinear}}$  in Eq.(3) include the monopole with the Dirac string and the anti-monopole, respectively. By the abelian projection  $A_\mu \rightarrow A_\mu \equiv A_\mu^3 T^3$ , the bilinear term, which is originated from the non-abelian nature, is dropped. The field-strength in the abelian projected QCD is derived as  $F_{\mu\nu} \equiv \partial_\mu A_\nu - \partial_\nu A_\mu + \frac{i}{e} \Omega [\partial_\mu, \partial_\nu] \Omega^\dagger$ , which breaks the abelian Bianchi identity. Thus, by the singular gauge transformation as  $\Omega$ , the monopole appears in the abelian sector of QCD.

Next, we consider monopole properties in terms of the action. In the static frame of the monopole with the magnetic charge  $g$ , a spherical ‘mag-

$$G_{\mu\nu}^\Omega = \underbrace{\partial_\mu A_\nu^\Omega - \partial_\nu A_\mu^\Omega}_\text{Abelian Projected QCD} + \frac{i}{e} \Omega [\partial_\mu, \partial_\nu] \Omega^\dagger + ie [A_\mu^\Omega, A_\nu^\Omega]$$

**Fig.5** Appearance of monopoles in abelian projected QCD.

netic field' is created around the monopole in the abelian sector of QCD as  $\mathbf{H}(r) = \frac{g}{4\pi r^3} \mathbf{r}$  with  $\mathbf{H}_i \equiv \epsilon_{ijk} \partial_j A_k^3$ . Then, the monopole inevitably accompanies a large fluctuation of the abelian gluon component  $A_\mu^3$  around it. For the abelian part  $S_{\text{Abel}} \equiv -\frac{1}{4} \int d^4x (\partial_\mu A_\nu^3 - \partial_\nu A_\mu^3)^2$  of the QCD action, the electro-magnetic energy created around the monopole is estimated as  $E(a) = \int_a^\infty d^3x \frac{1}{2} \mathbf{H}(r)^2 = \frac{g^2}{8\pi a}$ , where  $a$  is an ultraviolet cutoff like a lattice mesh. As the "mesh"  $a$  goes to 0, the monopole provides a large fluctuation of  $S_{\text{Abel}}$ , and hence the monopole seems difficult to appear if the abelian gauge theory is controlled by  $S_{\text{Abel}}$ . This is the reason why QED does not have the point-like Dirac monopole. Then, why can the monopole appear in the abelian sector of QCD? To answer it, let us consider the division of the total QCD action  $S_{\text{QCD}}$  into the abelian part  $S_{\text{Abel}}$  and the remaining part  $S_{\text{off}} \equiv S_{\text{QCD}} - S_{\text{Abel}}$ , which is contribution from the off-diagonal gluon component. Unlike  $S_{\text{QCD}}$  and  $S_{\text{Abel}}$ ,  $S_{\text{off}}$  is not positive definite and can take a negative value in the Euclidean metric. Then, around the monopole, the abelian action  $S_{\text{Abel}}$  should be partially canceled by the remaining off-diagonal contribution  $S_{\text{off}}$  such that the total QCD action  $S_{\text{QCD}}$  around the monopole does not become extremely large. Thus, we expect large off-diagonal gluon components around the monopole for cancellation with the large field fluctuation of the abelian part. Based on this analytical consideration, we study action densities around monopoles in the MA gauge using the lattice QCD.

On the SU(2) lattice, we measure the action densities  $\bar{S}_{\text{SU}(2)}$ ,  $\bar{S}_{\text{Abel}}$  and  $\bar{S}_{\text{off}}$ , which are the SU(2), the abelian and the off-diagonal parts, respectively. We show the probability distributions of  $\bar{S}_{\text{SU}(2)}$ ,  $\bar{S}_{\text{Abel}}$  and  $\bar{S}_{\text{off}}$  in Fig.6. (To be exact,  $\bar{S}$  is the averaged value over the neighboring links around a dual link<sup>5</sup>.) For the total distribution on the whole lattice, most  $\bar{S}_{\text{off}}$  are positive, and both  $\bar{S}_{\text{Abel}}$  and  $\bar{S}_{\text{off}}$  tend to take smaller values than  $\bar{S}_{\text{SU}(2)}$  owing to

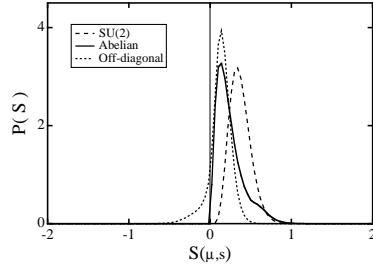


**Fig.6(a)** Probability distributions  $P(\bar{S})$  of the  $\bar{S}_{\text{SU}(2)}$  (dashed curve),  $\bar{S}_{\text{Abel}}$  (solid curve) and  $\bar{S}_{\text{off}}$  (dotted curve) in the MA gauge at  $\beta = 2.4$  on  $16^4$  lattice.

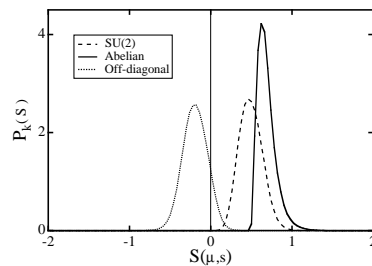


**Fig.6(b)** Probability distribution  $P_k(\bar{S})$  around the monopole for  $\bar{S}_{\text{SU}(2)}$ ,  $\bar{S}_{\text{Abel}}$  and  $\bar{S}_{\text{off}}$  in the MA gauge at  $\beta = 2.4$  on  $16^4$  lattice.

$\bar{S}_{\text{SU}(2)} = \bar{S}_{\text{Abel}} + \bar{S}_{\text{off}}$ . Around the monopole, however, the off-diagonal part  $\bar{S}_{\text{off}}$  of the action density tends to take a large negative value, and  $\bar{S}_{\text{off}}$  strongly cancels with the large abelian action density  $\bar{S}_{\text{Abel}}$  so as to keep the total  $\text{SU}(2)$  action small. Thus, monopoles can appear in the abelian sector in QCD without large cost of the QCD action due to the strong cancellation between the abelian action  $S_{\text{Abel}}$  and the off-diagonal part  $S_{\text{off}}$  of the action.

In conclusion, in the small distance, all  $\text{SU}(2)$  components contribute to the short-distance physics. In the dual-superconductor picture, the off-diagonal components are necessary to create the monopole in the abelian sector. In the large distance, however, the off-diagonal components are not necessary for the infrared physics, and only abelian gauge fields with monopoles describe the QCD vacuum.

#### 4 Monopole Condensation

In the dual Higgs theory, the monopole is assumed to be condensed, which has been suggested by the formation of the global network of the monopole current in the lattice QCD. In this section, we consider monopole condensation in the QCD-vacuum at the infrared scale. However, QCD is described by the gluon field not by the monopole current, and therefore it is difficult to clarify monopole condensation only with the lattice QCD simulation. To this end, we generate the monopole-current system on the lattice using a simple monopole-current action, and study monopole condensation and the role of the monopole to color confinement<sup>7</sup>.

In general, monopole-current action  $S[k_\mu(s)]$  includes the nonlocal Coulomb interaction as  $S_C = \int d^4x d^4y k_\mu(x) D(x-y) k_\mu(y)$  with the Coulomb propagator  $D(x)$ . In the dual Higgs phase, however, the effective interaction between monopole currents would be short-range due to the *screening effect* by the dual Higgs mechanism<sup>5,8,9</sup> similar to the Debye screening<sup>10</sup>. Then, the infrared partition functional of the monopole current  $k_\mu(x) \equiv k_\mu^3(x) \cdot \frac{\tau^3}{2}$  would be written as

$$Z = \int Dk_\mu \exp\left\{-\alpha \int_a d^4x \text{tr} k_\mu^2(x)\right\} \delta(\partial_\mu k_\mu), \quad (4)$$

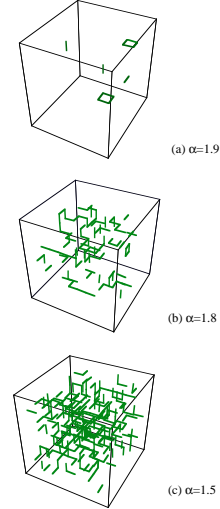


**Fig.7** Monopole current in the monopole-current system in  $\mathbf{R}^3$  at a fixed time.

where  $\alpha$  is the energy per unit length of the monopole current. Here,  $a$  is an ultraviolet cutoff larger than the screening length. We put the system on the 4-dimensional lattice with the lattice spacing  $a$ . Fig.7 shows behavior of the monopole current in the monopole current system for  $\alpha = 1.5, 1.8, 1.9$ . When energy  $\alpha$  becomes smaller, the monopole current is generated more easily. As  $\alpha = 1.5$ , the monopole current covers the whole lattice and creates the global network, which is similar to the monopole current in the QCD vacuum.

Here, let us consider this behavior of monopole currents in the analytical way. In the abelian gauge of QCD, the charge of the monopole is expected to be unity<sup>5</sup>. The partition function can be approximated as the single monopole-loop ensemble with the length  $L$ ,  $Z = \sum_L \rho(L) e^{-\alpha L}$ , where  $L$  and  $\rho(L)$  are length of the monopole loop and its configuration number, respectively. The monopole current with the length  $L$  is regarded as the  $L$  step self-avoiding random walk, where  $2d - 1 = 7$  direction is possible in each step. Therefore,  $\rho(L)$  is roughly estimated as  $(2d - 1)^L = 7^L$ , and the expectation value of the monopole-current length is found to be

$$\langle L \rangle = \frac{1}{Z} \sum_L \rho(L) L e^{-\alpha L} = \begin{cases} \{\alpha - \ln(2d - 1)\}^{-1} & \text{if } \alpha > \ln(2d - 1) \\ \infty & \text{if } \alpha < \ln(2d - 1). \end{cases} \quad (5)$$

When energy  $\alpha$  is larger than “entropy”  $\ln(2d - 1)$ , the monopole-loop length is finite. However, when  $\alpha$  is smaller than entropy, the monopole-loop length becomes infinite, which corresponds to monopole condensation in the current representation<sup>8</sup>. Here, the critical value on monopole condensation is  $\alpha_c \simeq \ln(2d - 1) \simeq \ln 7 \simeq 1.945$ , which corresponds to “entropy” of the self-avoiding random walk. Such a transition is quite similar to the Kosterlitz-Thouless transition in 2-dimensional superconductors, where vortex condensation plays an important role to the transition.

Next, we study how these monopole currents contribute to color confinement properties<sup>7</sup>. Quark confinement is characterized by the linear inter-quark potential, which can be obtained from area-law behavior of the Wilson loop,  $\langle W \rangle = \langle P \exp(i \epsilon \oint A_\mu dx_\mu) \rangle$ . The expectation value of the Wilson loop  $\langle W \rangle$  is shown in Fig.8. The Wilson loop exhibits the area law and the linear confinement potential:  $\ln \langle W \rangle$  decreases linearly with the quark loop area  $I \times J$ . Quantitatively, the string tension is measured by the Creutz ratio, and we show in Fig.9  $\chi(3, 3)$  as a typical example. For the monopole condensed phase as  $\alpha < \alpha_c$ , the string tension gets a finite value, while it vanishes for the non-condensed phase of monopoles as  $\alpha \geq \alpha_c$ . Thus, the confinement phase directly corresponds to the monopole condensed phase, and therefore monopole condensation is considered as essence of the confinement mechanism.

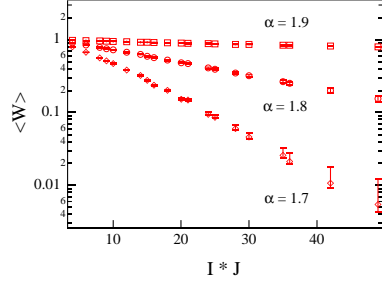


**Fig.8** The Wilson loop  $\langle W(I \times J) \rangle$  in the monopole-current system.

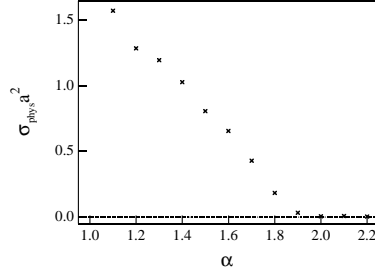


**Fig.9** The Creutz ratio as the function of  $\alpha$  in the multi-monopole system.

We compare the lattice QCD with the monopole-current system in terms of monopole condensation and confinement properties. The lattice QCD simulation shows that the QCD vacuum in the MA gauge holds the global network of the monopole-current. Considering the similarity on the monopole clustering, the QCD vacuum can be regarded as the monopole condensed phase with  $\alpha < \alpha_c$  in the monopole-current system, as shown in Fig.7(c). Such an identification of the QCD vacuum with the monopole condensed phase is also suggested in terms of the confinement properties, because the confinement phase corresponds to the monopole condensed phase as shown in Fig.7. Thus, monopole condensation is considered to occur at the infrared scale in the QCD vacuum and the confinement would be caused by monopole condensation there.

One of authors (H.I.) is supported by Research Fellowships of the Japan Society for the Promotion of Science for Young Scientists.

## References

1. Y. Nambu, Phys. Rev. **D10** (1974) 4262.
2. G. 't Hooft, Nucl. Phys. **B190** (1981) 455.
3. A. Di Giacomo, Nucl. Phys. **B** (PS) **47** (1996) 136 and references.
4. M. I. Polikarpov, Nucl. Phys. **B** (PS) **53** (1997) 134 and references.
5. H. Suganuma, H. Ichie, A. Tanaka and K. Amemiya Prog. of Theor. Phys. (Suppl.) (1998) in press; hep-lat/9804027, and references therein.
6. H. Ichie and H. Suganuma, Proc. of *Innovative Computational Methods in Nuclear Many-Body Problems (INNOCOM '97)*, hep-lat/9802032.
7. H. Ichie, A. Tanaka and H. Suganuma, Nucl. Phys. **B** (PS) 63A-C (1998) 468; H. Ichie, H. Suganuma and A. Tanaka Nucl. Phys. **A629** (1998) 82c.
8. Z. F. Ezawa and A. Iwazaki, Phys. Rev. **D25** (1982) 2681; **D26** (1982) 631.
9. A. Tanaka and H. Suganuma, Proc. of *INNOCOM '97* (World Scientific).
10. J. D. Stack, Nucl. Phys. **B** (Proc. Suppl.) **53** (1997) 524.